

Reactive Ion Beam Etching of Large Diffraction Gratings

B. Xu, S. D. Smith and D. J. Smith, Plymouth Grating Laboratory Inc., Plymouth, MA
D. Chargin, Fraunhofer USA, Center for Manufacturing Innovation, Boston, MA

Key Words: Reactive ion beam etching
Diffraction efficiency

Large area multilayer dielectric grating
Wavefront flatness

ABSTRACT

Large area Multilayer Dielectric (MLD) diffraction gratings are essential components for temporal pulse compression in high energy laser systems. MLD grating designs typically consist of a silica grating layer on top of a dielectric multilayer reflector. A reactive ion beam etching (RIBE) process using a gridded radio frequency (RF) ion source was developed to uniformly etch the silica grating layer through a binary photo-resist mask on large size optics. The reactive etching is performed in two steps to sequentially remove different layers of materials. The RIBE system utilizes a unique substrate translation mechanism to achieve a uniform etch on large optics. An optical photometer is used to monitor both the grating product and witnesses to determine the etch endpoints. Using this process, MLD diffraction gratings of 1740 lines/mm groove density on optics up to 920mm (length) \times 410mm (width) \times 100mm (thickness) have been uniformly etched with averaged diffraction efficiency greater than 85% and wavefront flatness less than 0.18 waves. While this process has been successful, there is a current etching problem which is discussed below.

INTRODUCTION

Large area diffraction gratings are required by the temporal pulse stretching and compression in high energy laser systems using chirped pulse amplification (CPA) technology [1]. The large aperture lasers (41cm \times 41cm) in those systems, and the high angle of incidence ($62^\circ - 72^\circ$) both require gratings as large as 1.5 meters in length and 0.5 meters in width. Traditionally, gold coated gratings have been employed in those systems due their high diffraction efficiency which is a result of the high reflectivity of the metal surface. However, as the interest grows in increasing the power density of the compressed beams, the absorption of a metal layer becomes a limiting factor in achieving high damage threshold. Thus, MLD diffraction gratings have been developed and fabricated to achieve both high diffraction efficiency and high laser damage threshold [2, 3]. Figure 1 shows the typical structure of a MLD grating before etching. It is composed of a multi-layer hafnia/silica high reflector coating topped with a binary photo-resist grating mask layer. An anti-reflection (ARC) layer is also sandwiched between high reflector and photo-resist layer interface to minimize the standing-wave effect during the holographic exposure.

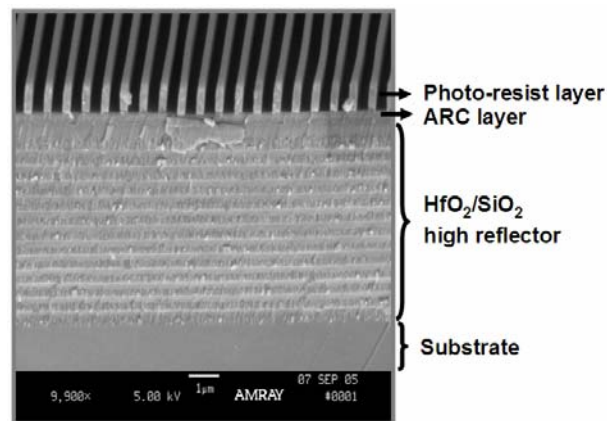


Figure 1: The scanning electron microscope (SEM) picture showing the cross section of a MLD grating before etching.

The large area MLD diffraction grating fabrication process developed at Plymouth Grating Laboratory (PGL) begins with the vacuum electron-beam deposition of the multi-layer high reflector coating on the optically flat substrate. The high reflector design uses the hafnia/silica material pair because of the high laser damage threshold and low coating stress that can be achieved with those materials using an optimized coating process [4]. The substrate is then uniformly coated with an anti-reflection layer and a photo resist layer using the meniscus coater and is baked overnight in a conventional oven.

The grating mask is first recorded in the photo-resist layer by a holographic exposure process performed using a novel grating patterning tool: the PGL Nanoruler. The resist is then developed by conventional means. The Nanoruler uses the scanning beam interference lithography (SBIL) technique originally developed at Space Nanotechnology Laboratory of the Massachusetts Institute of Technology (MIT) [5]. This technique interferes two coherent beams of approximately 1mm in size to produce a small grating image patch on the substrate. The grating image is exposed into one strip of photo-resist by moving the substrate along one direction (called one scan). By accurately switching many scans together, gratings can be written on large area substrates. This step-and-scan technique requires an extremely high level of fringe stability and accurate fringe motion relative to the moving substrate which is achieved using a high-performance heterodyne fringe-locking system. The Nanoruler is housed in an enclosure which protects it from a variety of environmental disturbances (heat, light, humidity variations, etc.) that destroy the high precision during grating exposure. Major advantages of the SBIL technique over other grating patterning tools include unlimited substrate size, as well as the capability of producing uniform dose and high contrast.

(a)

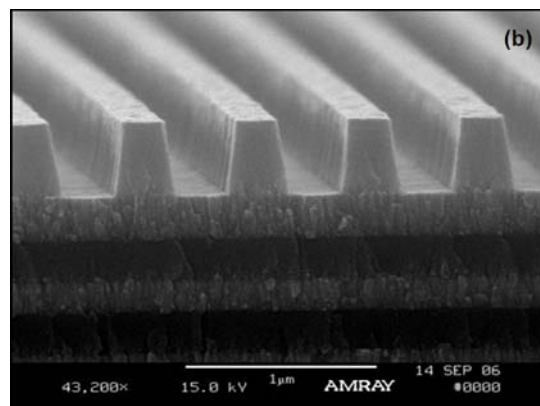
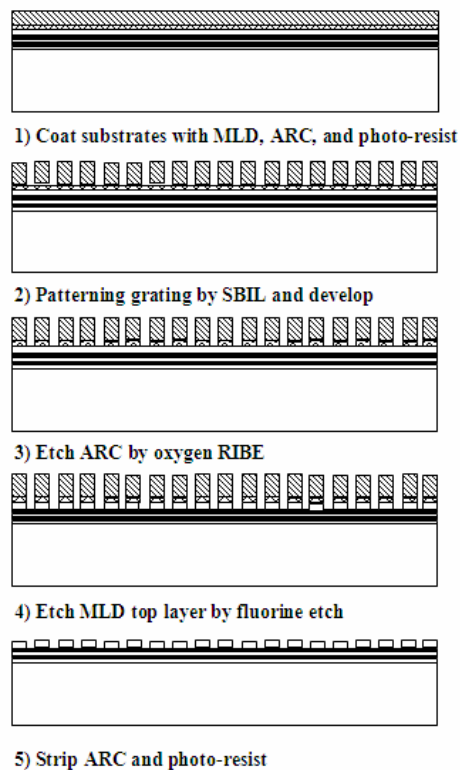
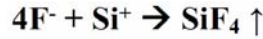


Figure 2: (a) The MLD grating fabrication steps, (b) the SEM picture of a grating etched into fused silica.

After the grating structure is developed into the photo-resist layer, a two-step reactive ion beam etching process is used to transfer it into the top silica layer of the high reflector. The ARC layer is reactively removed using a low-energy oxygen ion etching. Then the grating mask is selectively engraved into the silica layer using an ionized gas mixture of Trifluoromethane (CHF₃), argon, and oxygen. The fluorine species etches the silica by using the reaction given by



The volatility of the main etch product, silicon tetrafluoride (SiF₄), is very high and thus it can easily desorb from the etched surface. The chemical reaction and the etch selectivity can be significantly enhanced by the increased reactive species because of the physical bombardment of heavy argon ions on the grating groove bottom. Argon ions also mechanically remove the polymer layer which is the by-product of the chemical reaction.

After etching, an acid piranha cleaning is performed to chemically strip away the residual photo-resist, ARC, and the polymer layers formed during the reactive etching. The finished grating product is then subject to full-aperture metrology including the interferometry for the diffracted wavefront flatness and photometry for the diffraction efficiency measurement in the -1 order. Also, the witness gratings produced from the same fabrication batch are also cleaved and examined using an SEM. Figure 2 illustrates the complete MLD grating manufacturing process and includes a SEM picture of a finished witness grating are shown in Figure 2.

RIBE SYSTEM CONFIGURATION

The reactive ion beam etching for large area MLD diffraction gratings is performed in a multi-section stainless steel vacuum chamber. The dimensions of the main chamber and the x-y stage extension chamber make it suitable of etching sub-micron features on meter-size substrates. This etch chamber is equipped with a two-stage pumping system. The high vacuum level required by the etching process (~ 10⁻⁶ torr range) is achieved using two 10" cryo-pumps. A Veeco 16cm gridded RF ion source is installed on the chamber bottom and configured to supply a highly focused beam of ionized reactive gases to the moving substrates at an angle of 35°. An RF neutralizer is used to produce electrons for space charge balance and minimizing beam broadening at the substrate height. A unique single-belt drive XY stage is mounted on the chamber ceiling to translate the large size optics across the ion beam for uniform etching. An optical photometer is used to intermittently sample several specially prepared monitoring witnesses to determine etch endpoints.

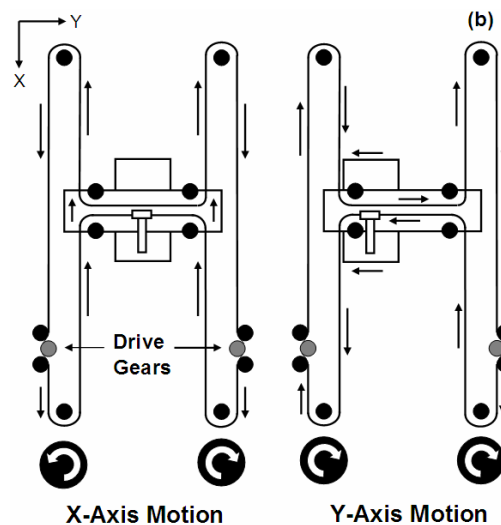
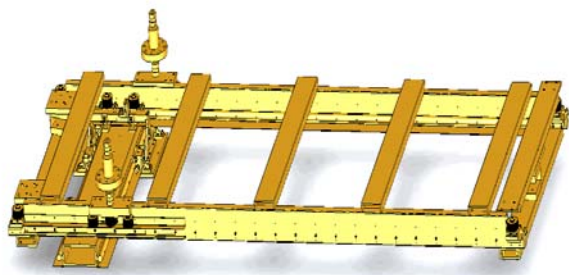


Figure 3: (a) The three dimensional SolidWorks® model showing the mechanical design of the XY stage. (b) The stage motions created by the single-belt drive.



The 16 cm gridded ion source uses a molybdenum 4-grid ion acceleration system. This system produces a significantly collimated ion beam as compared to the conventional 3-grid ion optics arrangement. The addition of a focus grid between the accelerator and decelerator grids reduces the overall ion beam divergence by combining the fast acceleration and deceleration of

ions after their extraction from the plasma discharge. The focus grid voltage needs to be optimized for the best beam collimation in various operation conditions. It is reported that the best collimation can be achieved when the focus grid voltage is adjusted to 2 to 3 times the total accelerating voltage which is the sum of the absolute values of the beam grid voltage and the accelerator grid voltage [6].

The mechanical structure of the custom designed XY translation stage is shown in Figure 3(a). The unique feature of this XY stage is that it utilizes a single-belt double-motor drive system, which allows the motors, gear boxes, and accompanying lubricants to be located outside the etch chamber. The driving belt itself is made of a polymeric material. The stage is mounted to the chamber ceiling using three flexure mounts to avoid chamber warping. The stage has a substrate handling capacity of greater than 100Kg and can run at a maximum speed of 250 mm/s with a position accuracy of less than 0.1mm. Figure 3(b) demonstrates schematically the creation of stage motion by varying the motor spinning direction and speed. To move the substrate in X axis two motors must spin in the opposite direction with the same speed, while for Y-axis motion, two motors have to rotate in the same direction using the same speed. Diagonal substrate movement is produced by spinning motors with varying speeds.

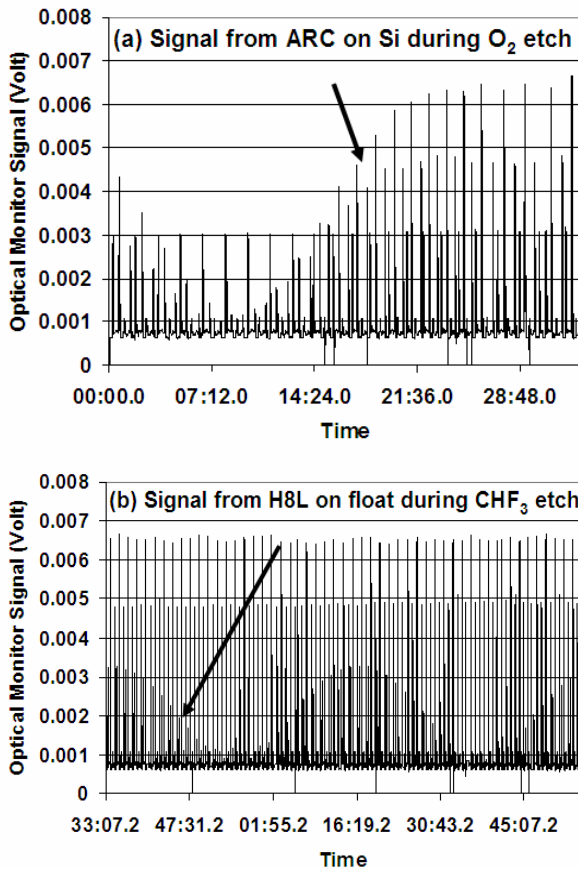


Figure 4: The intermittent optical photometer signals during (a) oxygen etch and (b) fluorine etch.

The optical photometer setup used in this RIBE system consists of a white light source, focusing optics, a mechanical chopper, optical fiber links, a monochromator, and a photo-detector. It is installed underneath the etcher and intermittently samples the reflection from the witnesses at one wavelength ($\lambda=500\text{nm}$) to determine the etch endpoints. Since the reactive etching of a grating is a 2-step process, two types of monitor witnesses are prepared. An ARC layer on a silicon wafer is used

to measure the ARC removal rate during the oxygen etch, and a 2-layer hafnia/silica (H8L design at 500nm) coating is used for monitoring the silica etch rate during the fluorine etch. To determine the etch depth, witnesses have to be strategically placed on the etch tooling to be frequently monitored by the optical photometer. Figure 4 shows the intermittent optical monitor signal as different layers of materials are being removed from the monitoring witnesses by the oxygen etch and the fluorine etch.

SUBSTRATE SCANNING SCHEMES AND RESULTS

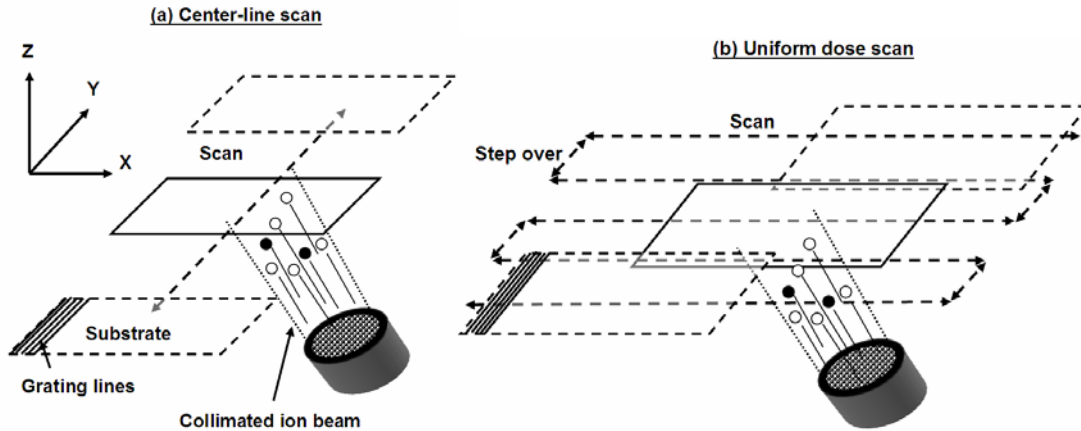
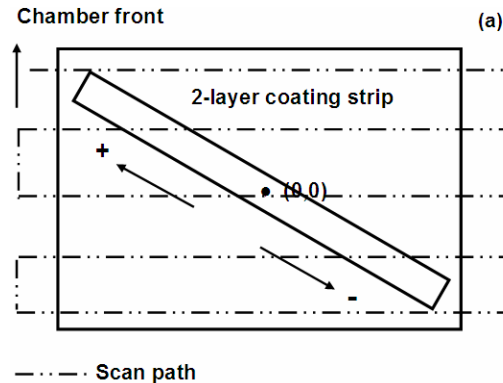


Figure 5: The schematic of two substrate scanning methods (a) center line scan (b) uniform dose scan.

Large-area substrates have to be scanned across the collimated ion beam to achieve the desired etch uniformity. Two types of substrate scanning methods have been developed, which are shown in Figure 5. The center line scan moves the substrate back and forth at a constant speed along the centerline of the beam. It is primarily used to optimize the ion source operation parameters and reactive gas flows because it allows quick sample setup and short development time. Once operation parameters are optimized using centerline scans, uniform dose scans are developed to achieve uniform material removal rates on large substrates. This scan scheme moves the substrate laterally across the ion beam at a constant speed and overlaps lateral scans by stepping over a short distance in the perpendicular direction.

Uniformity

Etch uniformity of the uniform dose scan is evaluated using a 1 meter long 2-layer hafnia/silica (H8L design at 500nm) coating strip. As shown in figure 6(a), it is attached along the diagonal of a rectangular etch tooling that simulates the meter-size grating product area. Scan parameters such as length, step-over size, scanning velocity are empirically tuned through a series of etch test runs. The uniformity result of a 3-hour fluorine reactive etching using the current uniform dose scan is shown in Figure 6(b). The etch depth is calculated every 3 cm along the coating strip. A fairly uniform etch rate is achieved with only 2% peak-to-valley etch thickness variations.



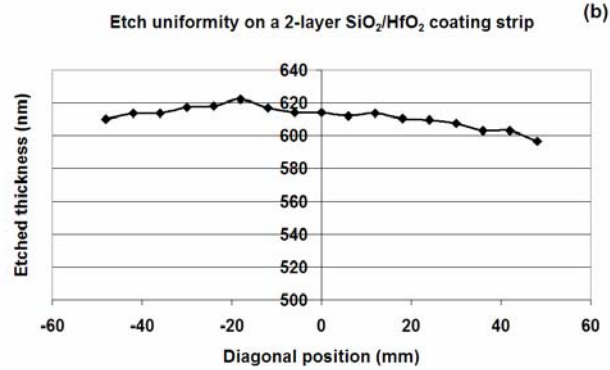


Figure 6: (a) Etch uniformity test sample setup and (b) uniformity results showing a 2% etched thickness variation for the 1-meter long etch sample.

Knowing the 2% etch thickness variation produced by the scanning method, a grating modeling study was performed using a grating modeling program named GSolver[®] to investigate the effect of etch depth on the -1 order diffraction efficiency. Grating diffraction efficiency is defined as the ratio of the diffracted beam energy to the incident beam energy. In typical pulse compression applications, the -1 order diffraction is evaluated. The results, in Figure 7(a), show that an incomplete etch of the top silica layer, indicated by the lower 3 curves, reduces the diffraction efficiency significantly. Conversely, a significant over-etch, indicated by the upper 3 curves, does not effect the diffraction efficiency. As shown in Figure 7(b) and 7(c), diffraction efficiency measurements on small witness gratings also agree with the modeling results.

Calibration

The optical monitor technique used in this system is an indirect monitoring method. As a result, a calibration needs to be established to achieve the correct etch depth on gratings. During the calibration the etch process is ended based on the optical monitor signal level. The etch length is adjusted based on the etched depth on witness gratings from the previous test run obtained by the ex-situ SEM analysis. The iteration continues until the correct etched thickness is achieved on witness gratings.

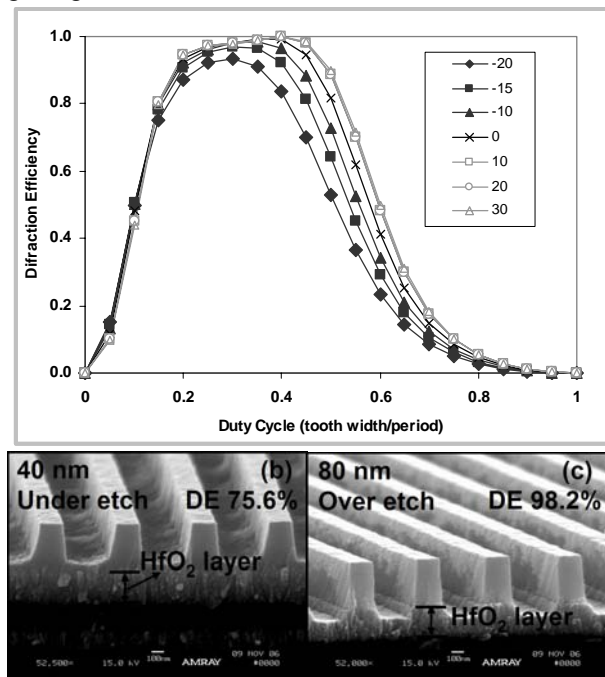


Figure 7: (a) The grating diffraction efficiency (DE) as a function of duty cycle for different etch depths. Under-etching of the grating has a much more severe effect on DE than over-etching does. (b) SEM of an under-etched grating and measured diffraction efficiency (c) SEM of an over-etched grating sample and measured diffraction efficiency.

Etching results on large size optics

PGL has successfully etched MLD diffraction gratings (groove density of 1740 lines/mm for 1054nm) on three large-size optics including one 42cm x 21cm x 10cm thick optic and two full scale optics which are 92cm x 42cm x 10cm thick. After etching and subsequent piranha cleaning, the performance of these gratings was examined in terms of the -1 order diffraction efficiency and the wavefront flatness of the diffracted beam. The diffraction efficiency was measured using a scanning laser photometer operated at 1053nm. The three etched gratings exhibited the averaged diffraction efficiency of 95%, 90% and 85% respectively. The diffraction efficiency maps of the subscale optics and one full-size optics are shown in Figure 8. The diffracted wavefront flatness was evaluated on a full-aperture phase-shifting interferometer in both the ambient and the dry-nitrogen purged environment which simulates the grating use condition in a vacuum. The diffracted beam is measured at the Littrow angle (72.5° at 1054nm) for both the clockwise and counter clockwise grating orientations with respect to the incoming measuring beam. Figure 9 shows the diffracted wavefront measurement of one etched full-scale grating in the clockwise orientation. The overall peak to valley of 0.173 waves is excellent considering the size of the optic.

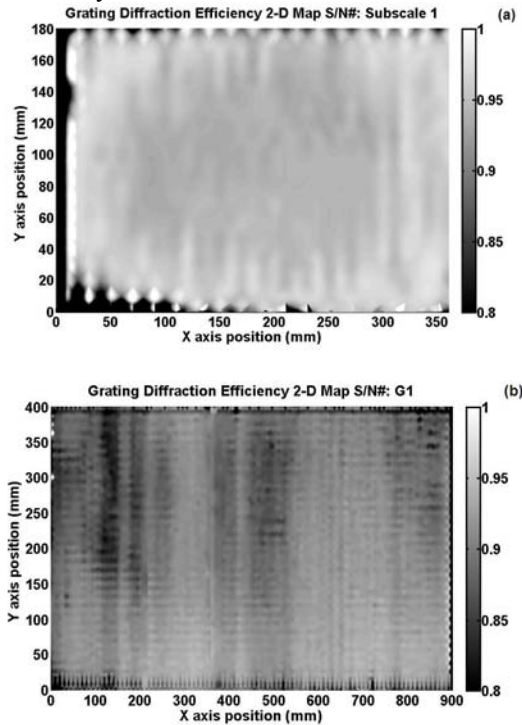


Figure 8: The diffraction efficiency maps of two large size gratings: (a) subscale optic and (b) full-scale optic GR1.

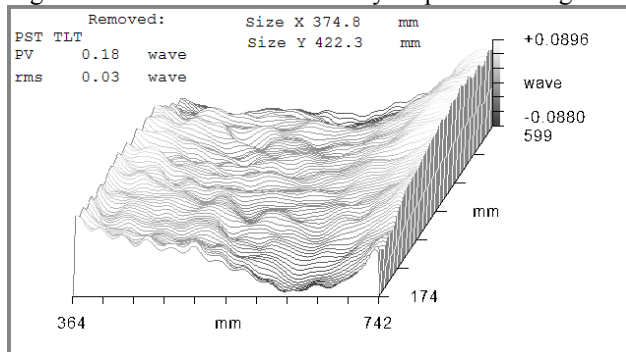


Figure 9: The wavefront (at 1054nm) flatness measurement of one full scale grating at the Littrow angle ($\lambda = 1054\text{nm}$).

Current etching problem

Large optics, with their large surface areas to etch, present a larger load of reactants and etch products than typically seen in reactive etch chambers. Additionally, a large optic has a much different thermal mass than the thin witnesses preferred for

SEM analysis. These scale-up issues became apparent in the early production batches of gratings. After several weeks of large-scale runs, the silica etching stopped. The problem was identified during the diffraction efficiency measurement of several full-scale gratings recently etched using the previously successful recipe. Both product grating and the witnesses from the same grating batch were measured. The full-scale gratings yielded a significantly lower average diffraction efficiency of less than 30%, while all the witness gratings measured an average diffraction efficiency of >90%. One theory for this discrepancy in diffraction efficiency is that a layer of excessive polymer, produced during etching, is covering the surface of the large gratings. This layer eventually terminates the fluorine etching process resulting in an incomplete etch and a low diffraction efficiency.

At the time of this writing these issues are still being investigated. This problem is typical of scale-up problems, where issues of vacuum system loading may never be seen with small samples but will become dominant when applied to the large scale device.

CONCLUSION

A Reactive Ion Beam Etching process using a gridded RF ion source has been developed to etch MLD gratings on large area optics. Substrate scanning methods have been designed using a unique XY translation system to achieve uniform etch and an optical photometer has been used to determine the etch endpoints. MLD diffraction gratings on optics up to 920mm (length) × 410mm (width) × 100mm (thickness) have been uniformly etched. Good diffraction efficiency and excellent wavefront flatness were achieved. Future work will focus on solving the incomplete etching problem on large optics.

ACKNOWLEDGEMENT

Authors wish to acknowledge the financial support for this work from the Institute of Laser Engineering at University of Osaka and Hakuto LTD. in Japan, technical assistance was provided by Dr. Mark Schattenburg of MIT, Mike McCullough, Don Hiller, Troy Booker and Mike Bird, all from Plymouth Grating Laboratory, Inc..

REFERENCES

1. D. Strickland and G. Mourou, "Compression of amplified chirped optical pulses", *Optical Communications*, 56, 219-221, (1985)
also,
S. Backus, C. G. Durfee III, M. M. Murnane and H. C. Kapteyn, "High power ultrafast lasers", *Review of Science Instruments*, Vol. 69, pp.1207-1223, 1998.
2. M.D. Perry, R.D. Boyd, J.A. Britten, D. Decker, B.W. Shore, C. Shannon, E. Shults, and L. Li. "High Efficiency Multilayer Dielectric Diffraction Gratings", *Optics Letters*, 20, 940-942, (1995)
3. M.D.Perry, J.A. Britten, H.T. Nguyen, R.D. Boyd, B.W.Shore, "Multilayer Dielectric Diffraction Gratings", U.S. Patent no. 5907436, (1999)
4. D. J. Smith, C. M. Smith, D. Hiller, and S. D. Smith, "Reducing the stress of hafnia/silica multilayers with ion-assisted deposition for use in high-power diffraction gratings" *49th Annual Technical Conference Proceedings of Society of Vacuum Coaters*, pp.421-425, 2006
5. M. Schattenburg and P. N. Everett, "A method and system for interference lithography using phase locked scanning beams", U.S. Patent 6882477 B1
6. E. K. Wahlin, M. Watanabe, J. Shimonek, D. Burtner and D. Siegfried, "Enhancement of collimated low-energy broad-beam ion source with fourth-grid accelerator system", *Applied Physics Letters*, Vol. 83, pp.4722-4724,2003